

Harmonic Pollution Control of the Electrical Network by Three-Phase Shunt Active Filter: Comparative Study of Controls, by Hysteresis and by Duty Cycle Modulation

T. Patrice Nna Nna, S. Ndjakomo Essiane, S. Pérabi Ngoffé, F. Amigue Fissou

Abstract—This paper deals with the harmonic decontamination of current in an electrical grid by an active shunt filter in order to improve power quality. The contribution of this paper is mainly based on the proposal of a control strategy for an active filter based on Duty Cycle Modulation (DCM). First, three-monophase method is applied for the identification of disturbing currents. A Simulink model of this method is given for one phase of the grid. Secondly, two orders were designed: the first one is the Hysteresis Control and the second one is the DCM Control. Finally, a comparative study of the two controls was performed. The results obtained show a significant improvement in the rate of harmonic distortion for both controls. The harmonic distortion for the Hysteresis control is limited by the non-controllability of the switching frequencies of the inverter's switches and reduces the harmonic distortion rate (THD) to 3.12% as opposed to the DCM control which limits the THD to 2.82% which makes it better.

Keywords—Harmonic pollution, shunt active filter, hysteresis, Duty Cycle Modulation.

I. INTRODUCTION

THE advent of semiconductor components has made it easier to supply domestic and industrial appliances with electrical energy using converters. It should be noted, however, that the increasing use of power electronics components in electrical networks is not without consequences for power quality [1]. Indeed, the connection of power electronic devices (fluorescent lighting fixtures, computer equipment, domestic appliances) with non-linear characteristics to electrical networks causes pollution of the latter through harmonic currents or voltages [2]. These harmonic components are the cause of the malfunctions observed in the electrical network when the rate of harmonic distortion (THD) no longer complies with the standards.

Théodore Patrice Nna Nna is a graduate Student in the PhD training program of the Training Unit for Applied Sciences of the postgraduate school for Pure and Applied Sciences of University of Douala and is assistance teacher of University of Maroua, Cameroon (e-mail: etknna@yahoo.fr).

Salomé Ndjakomo Essiane is with the Laboratory of Applied Engineering and Biotechnology, HTTTC of EBOLOWA, University of Yaoundé I Cameroon (e-mail: salomendjakomo@gmail.com).

Stève Pérabi Ngoffé works in the Department of Electrical Engineering of the IUT, University of Douala, Cameroon (e-mail: ngoffeperabi@yahoo.fr).

Filbert Amigue Fissou is a graduate Student in the PhD training program of the Training Unit for Applied Sciences of the postgraduate school for pure and applied sciences of university of Douala Cameroon (e-mail: fulbertfissou@yahoo.fr).

The frequency range corresponding to the study of harmonics is generally between 100 and 2000 Hz, i.e. from the 2nd harmonic to the 40th harmonic, the amplitudes of these harmonics generally decrease with frequency [3] and the mains frequency is 50 Hz. Harmonics have many effects on electrical installations [4], [5], including heating and malfunctioning of some equipment, interference with telecommunication networks, the risk of resonance excitation, etc. [4]-[7].

The decontamination of electrical networks by eliminating harmonics has long been a concern of research in electrical engineering and electronics. Several solutions have been proposed, including the use of filters. Passive filters, which are couplings of capacitors and inductors, prevent harmonic currents from propagating in power networks and compensate for reactive power [6]. However, these filters lack adaptability to changes in network impedance and load impedance [7]. Active filters, the principle of which is illustrated in (Fig. 1), consist of injecting into the polluted network harmonic currents or voltages of the same amplitude as the polluting harmonics but in phase opposition with them. The use of active filters avoids the disadvantages of passive filters. Three topologies are used in this respect, the serial active filter (FAS), the parallel or shunt active filter (FAP) and the hybrid active filter (FAH). The FAP is the most widely used solution for the decontamination of harmonic currents, and several research projects have been carried out on the control of the filter from its average model [2] or the direct and hybrid control, the linear and non-linear control [8].

There are many FAP control strategies [7] but the differences lie in the THD reduction performance, the quality of the obtained wave, the simplicity of the scheme and the cost. The latter will be used in this article.

Active filtering can be single-phase or three-phase depending on whether the network to be cleaned is single-phase (domestic networks) or three-phase (industrial networks), with a voltage or current structure and whether the storage element of the active filter is capacitive or inductive. It can also be in series or parallel (shunt) depending on the harmonics to be eliminated (of voltages or currents respectively).

In the control of active filters, pulse width modulation (PWM) and hysteresis modulation are widely used. PWM has been applied in [9], [10] and has proven performance due to

its immunity to noise, its effectiveness in harmonic pollution control but it has limiting dynamic properties, the system response to abrupt changes in reference signals is slow and the implementation is complex. The second [11], [12] has been shown easy to implement, robust and does not require extensive knowledge of the model of the system to be controlled or its parameters. Its major disadvantage is that it does not allow the switching frequency of the semiconductors to be controlled. These two controls have been compared in [1], [7] and it appears that the hysteresis control seems to be better for the harmonic control of power networks than the PWM control and will be used in this paper with the network parameters of [7].

DCM control [13]-[15] is a promising solution for industrial process control. The non-inverter mounted Duty Cycle Modulator is the most widely used in converter control and has been applied in [15]-[17]. This modulator is based on the non-linear operation of an operational amplifier. Its simplicity of implementation, simple mathematical foundations and spectral poverty are real assets. This modulator will also be used in this paper.

In this article a comparative study and simulation is performed between the Hysteresis and the DCM control of the inverter of a three-phase shunt active filter for a harmonic pollution control application. First, a method based on the identification and determination of reference currents using the three-monophas method is proposed. Secondly, the reference currents are used to control the power switches of the active filter [18], respectively by Hysteresis and DCM. The main contribution of this work is mainly based on the proposal of a control strategy for an active filter based on DCM for harmonic pollution control.

II. METHOD

We propose a method whose active filter command strategy is based on the three-phase method, which allows the identification and determination of reference currents. These reference currents are then injected into the DCM, which generates the control commands for the inverter and then the LC filter serves as a coupling between the grid and the active filter. The currents from the filter are then fed into the grid in antiphase.

A. Principle and Structure of the Active Shunt Filter

The principle of the active filter consists in injecting into the polluted network harmonic currents or voltages of the same amplitude as the polluting harmonics but in phase opposition with them.

Fig. 1 describes the general structure of the three-phase voltage type active shunt filter. It consists of a power part and a control part. The power part generally comprises a voltage inverter based on power switches controllable on and off with antiparallel diodes, an energy storage circuit (capacitive in our study) and an output filter.

B. Identification of Disturbing Currents by the Three-Monophas Method

The algorithm executed by the three-monophas method [1] for the identification of disturbance currents for one of the phases is given in Fig. 2.

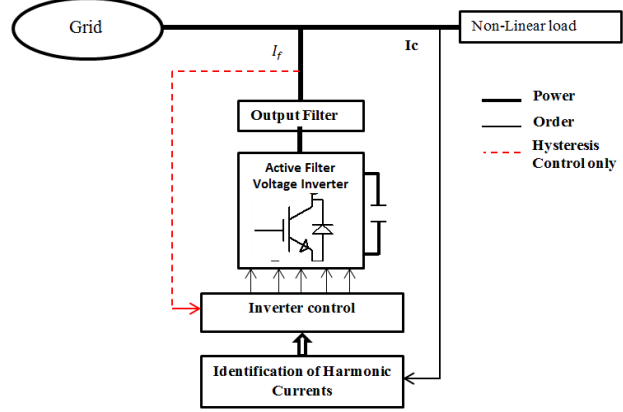


Fig. 1 General structure of the active three-phase voltage-type shunt filter

The principle of the three-monophas method is based on the estimation of the amplitude of the fundamental active and reactive components of the current (I_c) absorbed by the load. This method is applicable to single-phase and three-phase systems and allows the three phases to be treated independently.

For a current absorbed by the non-linear load, the components for each phase are given by the relations:

$$I_{ca}(t) = \sum_{k=1}^{+\infty} I_{cah} \sin(h\omega t - \varphi_{ak}) = I_{ca1} \sin(\omega t - \varphi_{a1}) + \sum_{k=2}^{+\infty} I_{cah} \sin(h\omega t - \varphi_{ak}) \quad (1)$$

$$I_{cb}(t) = \sum_{k=1}^{+\infty} I_{cbh} \sin(h\omega t - \varphi_{bk}) = I_{cb1} \sin(\omega t - \varphi_{b1}) + \sum_{k=2}^{+\infty} I_{cbh} \sin(h\omega t - \varphi_{bk}) \quad (2)$$

$$I_{cc}(t) = \sum_{k=1}^{+\infty} I_{cch} \sin(h\omega t - \varphi_{ck}) = I_{cc1} \sin(\omega t - \varphi_{c1}) + \sum_{k=2}^{+\infty} I_{cch} \sin(h\omega t - \varphi_{ck}) \quad (3)$$

Or, I_{ca1} , I_{cb1} , I_{cc1} represent the amplitudes of fundamental currents each phase and φ_{a1} , φ_{b1} , φ_{c1} the phase shifts between the currents of the fundamental.

A phase-locked loop (PLL) is used to calculate the fundamental pulses in order to avoid erroneous interference currents.

$$I_{ca}(t) \cdot \sin(\omega t) = I_{ca1} \sin(\omega t - \varphi_{a1}) \cdot \sin(\omega t) + \sin(\omega t) \cdot \sum_{k=2}^{+\infty} I_{cah} \sin(h\omega t - \varphi_{ak}) \quad (4)$$

$$I_{ca}(t) \cdot \cos(\omega t) = I_{ca1} \sin(\omega t - \varphi_{a1}) \cdot \cos(\omega t) + \cos(\omega t) \cdot \sum_{k=2}^{+\infty} I_{cah} \sin(h\omega t - \varphi_{ak}) \quad (5)$$

We then obtain:

$$I_{ca1} \sin(\omega t - \varphi_{a1}) \cdot \sin(\omega t) = \frac{I_{ca1}}{2} [\cos(\varphi_{a1}) - \cos(2\omega t -$$

$$\varphi_{a1})] + \sin(\omega t) \cdot \sum_{k=2}^{+\infty} I_{cah} \sin(h\omega t - \varphi_{ak}) \quad (6)$$

$$I_{ca1} \sin(\omega t - \varphi_{a1}) \cdot \cos(\omega t) = \frac{I_{ca1}}{2} [-\sin(\varphi_{a1}) + \sin(2\omega t - \varphi_{a1})] + \cos(\omega t) \cdot \sum_{k=2}^{+\infty} I_{cah} \sin(h\omega t - \varphi_{ak}) \quad (7)$$

Equations (6) and (7) show that only the DC components are proportional to the amplitude of the active fundamental current and the reactive fundamental current respectively. The first AC components have a frequency equal to twice the main frequency. These are filtered using a low-pass filter with a relatively low cut-off frequency to prevent low-frequency ripple at the output. However, a good compromise between efficient filtering of spurious frequencies and fast dynamics of the extraction algorithm is not available. Equations (8) and (9) are obtained after filtering.

$$[I_{ca1} \sin(\omega t - \varphi_{a1}) \cdot \sin(\omega t)]_{filtered} = \frac{I_{ca1}}{2} \cos(\varphi_{a1}) \quad (8)$$

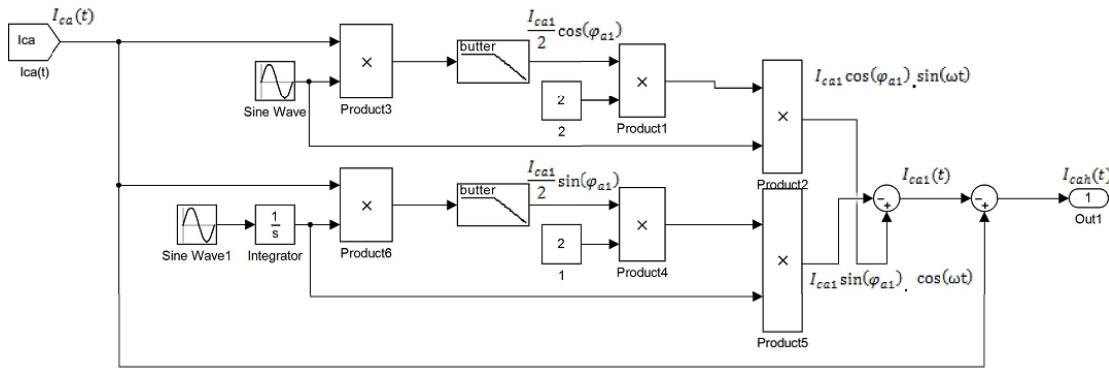


Fig. 2 Algorithm of the three-monophas method

C. Hysteresis Control

The capacity and adaptability of an active filter lies in the effectiveness of the control of the switches of the inverter that makes it up. There are two control techniques using hysteresis: modulated hysteresis control, which is rather complex to implement, and conventional hysteresis control.

Conventional hysteresis control is very commonly used due to its ease of use and robustness, it has been chosen for this work. This control strategy ensures satisfactory control of the current without requiring extensive knowledge of the model of the system to be controlled or its parameters. Fig. 3 explains its principle, which consists in first establishing the error signal, the difference between the reference current I_f^* and the current produced by the inverter I_f . This error is then compared with a template called a hysteresis band to determine the control commands for the switches [7], [19].

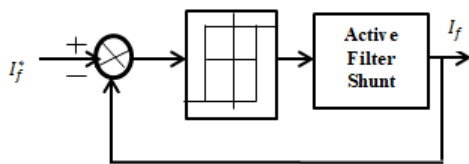


Fig. 3 Conventional hysteresis control

$$[I_{ca1} \cos(\omega t - \varphi_{a1}) \cdot \cos(\omega t)]_{filtered} = \frac{I_{ca1}}{2} \sin(\varphi_{a1}) \quad (9)$$

By multiplying (8) and (9) by 2 and then by $\sin(\omega t)$ and $\cos(\omega t)$ respectively, the fundamental current $I_{ca1}(t)$ is reconstituted :

$$I_{ca1}(t) = I_{ca1} \cos(\varphi_{a1}) \cdot \sin(\omega t) - I_{ca1} \sin(\varphi_{a1}) \cdot \cos(\omega t) \quad (10)$$

The harmonic currents $I_{cah}(t)$ on phase (a) are obtained by subtracting the fundamental $I_{ca1}(t)$ from the total current $I_{ca}(t)$.

The three fundamental voltages at the connection points of the FAP are equal but phase-shifted from $2\pi/3$.

Once the disturbance currents have been identified, the second phase of the control of the active shunt filter consists of determining its impurities.

D. Modulation Control with DCM

Several schemes of DCMs exist and have been developed, however the non-inverter mounted Cyclic Ratio Modulator is the most widely used in the control of converters [15]-[17]. Fig. 4 shows its operating principle which consists in varying the duty cycle as a function of the modulated signal I_{ref} injected at the input of the modulator thanks to an excellent developed linear approximation of the duty cycle by correctly setting the modulator parameters.

For this paper we use the DCM with optimal non-inverting mounting.

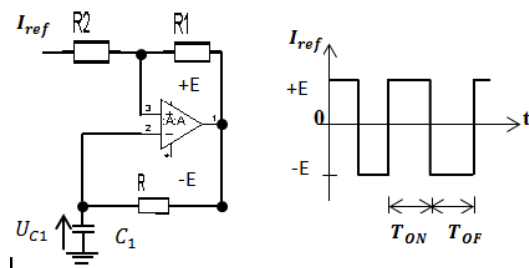


Fig. 4 Current control by DCM

Equations (15) and (16) reflect the mathematical model of the DCM; the duty cycle is defined in (21). An excellent linear approximation of (21) using the tangent plane method has found the numerical values $R_1 = R = 10K\Omega$; $R_2 = 8.87K\Omega$; $C = 330\eta F$ for which the signal I_{ref} presented at the input of the modulator is transformed into a switching wave. At the non-inverting input of the operational amplifier, we have:

$$u^+ = \frac{\frac{X_{ref}}{R_1} + \frac{U_s(t)}{R_2}}{\frac{1}{R_1} + \frac{1}{R_2}} \quad (11)$$

and

$$I_{ref} = X_{ref} \Rightarrow u^+ = \frac{X_{ref}R_2}{R_1+R_2} + \frac{U_s(t)R_1}{R_1+R_2} \quad (12)$$

with:

$$\alpha = \frac{R_1}{R_1+R_2} \quad (13)$$

$$1-\alpha = \frac{R_2}{R_1+R_2} = \alpha_1 \quad (14)$$

The operational amplifier (AOP) in Fig. 4 operates in switching and the output signal assumes two states according to the conditions imposed by u^+ and u^- , we have:

$$\Rightarrow u^+ = \begin{cases} E & \text{si } u^+ > u^- \\ -E & \text{si } u^+ < u^- \\ \alpha E + \alpha_1 X_{ref} & \text{si } U_s(t) = E \\ -\alpha E + \alpha_1 X_{ref} & \text{si } U_s(t) = -E \end{cases} \quad (15)$$

The capacitor voltage variation is defined by:

$$RC \frac{dU_c(t)}{dt} + U_c(t) = U_s(t) \quad (16)$$

Hence

$$U_c(t) = (u_i - u_f)e^{-t/\tau} + u_f \quad (17)$$

The charging and discharging time of the capacitor are included respectively: $0 < t < T_1$ and $T_1 < t < T_2$

$$T_1 = -\tau \ln \frac{\alpha_1 X_{ref} + (\alpha-1)E}{\alpha_1 X_{ref} - (1-\alpha)E} \quad (18)$$

and

$$T_2 = -\tau \ln \frac{\alpha_1 X_{ref} - (\alpha-1)E}{\alpha_1 X_{ref} + (1+\alpha)E} \quad (19)$$

$$\begin{aligned} T &= \tau \ln \frac{\alpha_1 X_{ref} - (1+\alpha)E}{\alpha_1 X_{ref} + (\alpha-1)E} + \tau \ln \frac{\alpha_1 X_{ref} + (1+\alpha)E}{\alpha_1 X_{ref} - (\alpha-1)E} \\ \Rightarrow T &= \tau \ln \left(\frac{(\alpha_1 X_{ref})^2 - ((1+\alpha)E)^2}{(\alpha_1 X_{ref})^2 - ((\alpha-1)E)^2} \right) \end{aligned} \quad (20)$$

The duty cycle $R_m(X_{ref})$:

$$R_m(X_{ref}) = \frac{T_1(X_{ref})}{T(X_{ref})} \quad (21)$$

$$\Rightarrow R_m(X_{ref}, \alpha, E) = \frac{\ln \frac{\alpha_1 X_{ref} - (1+\alpha)E}{\alpha_1 X_{ref} + (\alpha-1)E}}{\ln \left[\frac{(\alpha_1 X_{ref})^2 - ((1+\alpha)E)^2}{(\alpha_1 X_{ref})^2 - ((\alpha-1)E)^2} \right]} \quad (22)$$

In order to improve the efficiency of the electronic parts of the non-inverting MRC modulator, we are optimizing our modulator. The aim is to find the optimal characteristic parameters α , τ and E of the modulator providing an excellent level of operation. For this purpose, the effects of non-linearity and variation of the characteristic parameters were studied. The optimal quality of the modulator obtained is observed through its characteristic quantities: $R_m(X_{ref}, \alpha, E)$ and $f_m = \frac{1}{T(X_{ref}, \alpha, E, \tau)}$ with f_m being the frequency of the modulator and $R_m(X_{ref}, \alpha, E)$ the duty cycle.

Optimizing the MRC modulator therefore means maximizing $P_m(\alpha, E)$ or minimizing $-P_m(\alpha, E)$ which is the slope. Our optimisation criterion is therefore $P_m(\alpha, E)$ or

$$P_m(\alpha, E) = \frac{\alpha}{E(1+\alpha) \log \left(\frac{1+\alpha}{1-\alpha} \right)} \quad (23)$$

The constraints governing the optimization problem are:

$$\begin{cases} f_{m0} = \frac{1}{2\tau \ln \left(\frac{1+\alpha}{1-\alpha} \right)} \\ f_{min} = \frac{1}{\tau \ln \left[\frac{(\alpha_1 X_{max})^2 - ((1+\alpha)E)^2}{(\alpha_1 X_{max})^2 - ((\alpha-1)E)^2} \right]} \\ 0 < \alpha < 1 \end{cases} \quad (24)$$

With the basic frequency of the modulator f_{m0} previously selected, the minimum frequency f_{min} previously established and $f_{min} > f_{mlim}$, with f_{mlim} is the limit modulator frequency.

Our work on optimization is based on the formulation given in [20] and for the chosen f_{m0} equal to 200 KHz, the frequency f_{mlim} is obtained by calculating f_{min} for α very small.

We obtain the following optimum parameters of DCM:

$$\begin{aligned} \Rightarrow \alpha &= 0.003081723734398 \text{ or } \alpha = \frac{R_1}{R_1+R_2} \text{ and } 1-\alpha = \frac{R_2}{R_1+R_2} = \alpha_1 \\ \Rightarrow \tau &= 0.000486670905896s \text{ ou } \tau = RC \end{aligned}$$

This allows the choice of the following parameters: $R_1 = 330\Omega$; $R = 1K\Omega$; $R_2 = 10K\Omega$; $C = 47\eta F$; for $E = 12V$.

E. Harmonic Distortion Rate (THD)

The evaluation of current harmonics in an electrical network involves calculating the rate of harmonic distortion by applying (25):

$$THD = \sqrt{\frac{\sum_{n=2}^{\infty} I_{n,eff}^2}{I_{1,eff}^2}} \quad (25)$$

III. RESULTS AND DISCUSSION

A. Results

Our results are of three kinds and presented for one phase (a): first we give the results of the simulations of the power grid without filter, then the results of the simulations with filter connected for conventional hysteresis control and finally the results of the simulations with filter connected for DCM control.

The simulated electrical network is three-phase three-wire and the MATLAB/Simulink software is used [6].

The pollutant load is a conventional three-phase rectifier connected in series in an electrical network [6]. Fig. 5 is the Simulink model of DCM.

The general structure of the studied system is given in Fig. 6, the system is constituted:

- A three-phase power source,
- A non-linear charge,
- An active three-phase shunt filter connected in parallel to the mains,
- A filter control unit.

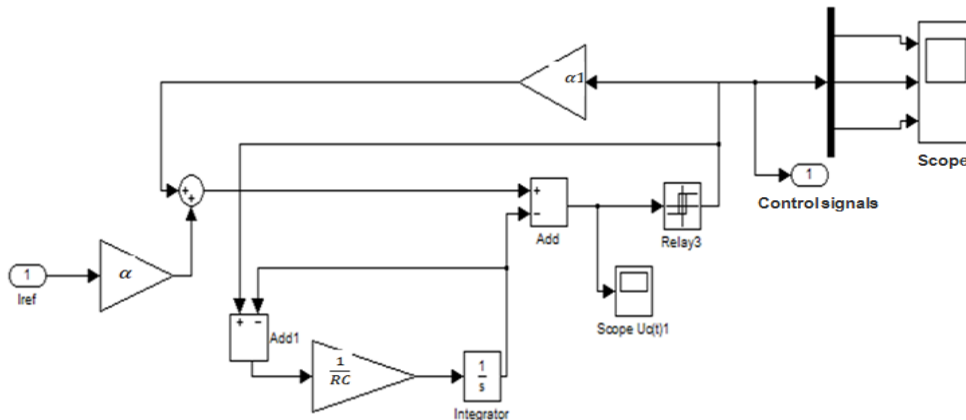
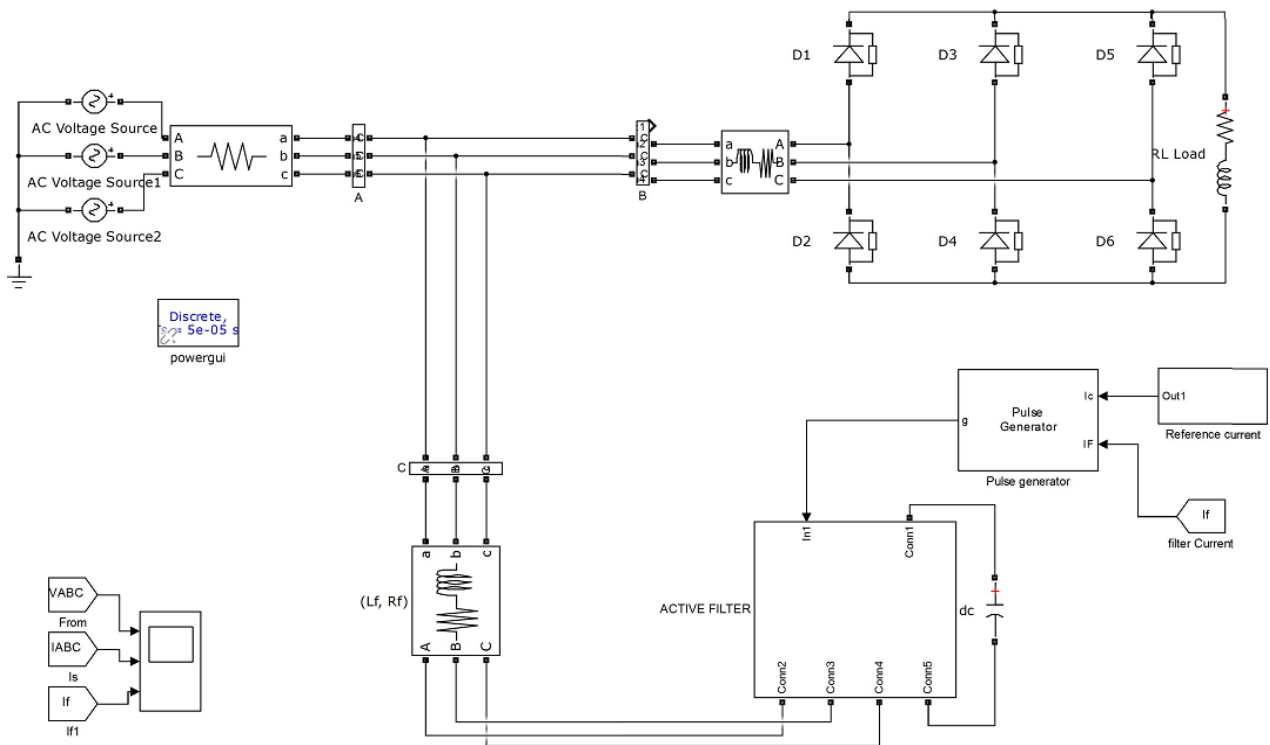


Fig. 5 Simulation diagram of the DCM



(a) Conventional Hysteresis Control

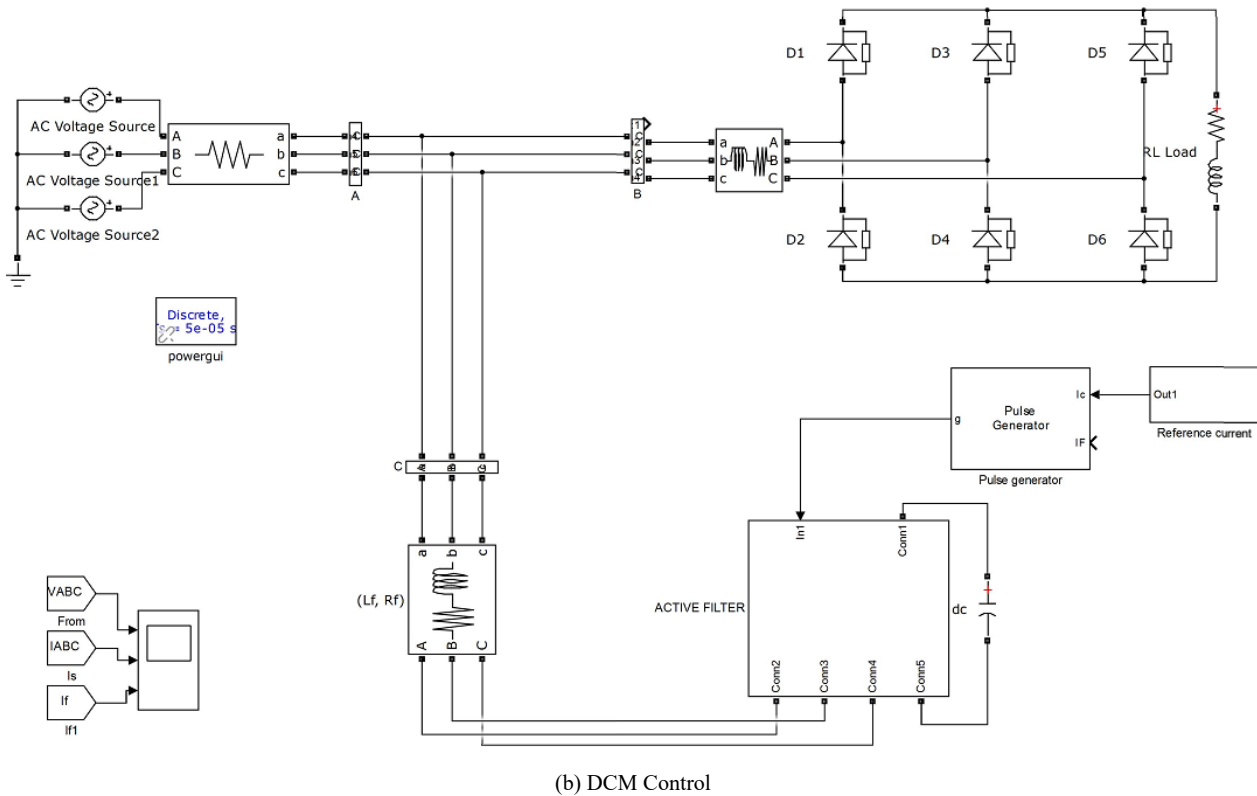


Fig. 6 Simulation diagrams

Simulation parameters are grouped in Table I.

TABLE I SIMULATION PARAMETERS	
DCM	$\alpha = 0.003081723734398$, $\tau = 0.000486670905896s$
Source	$V_s = 240V$, $f = 50Hz$, $R_s = 3,5m\Omega$,
Load	$L_c = 0,023 mH$, $R_c = 0,82m\Omega$, $R_d = 0,78m\Omega$, $L_c = 2,6 mH$
Filter	$R_f = 5m\Omega$, $L_f = 0,15 mH$, $C = 8 mF$,
H (Width of hysteresis window)	2A

a. For the Electricity Network

Fig. 7 shows the course of the current I_{sa} in the network before filtering for phase (a), the spectral analysis of this current is presented in Fig. 8 and we observe the presence of several ranks of harmonics disturbing the current waveform, i.e. a THD of 26.57%.

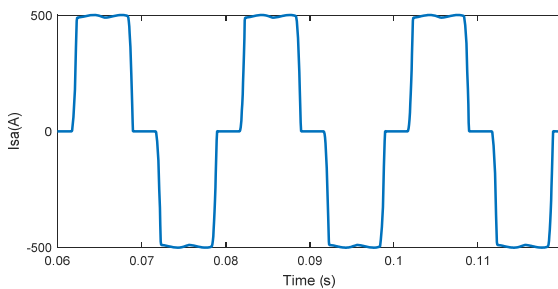
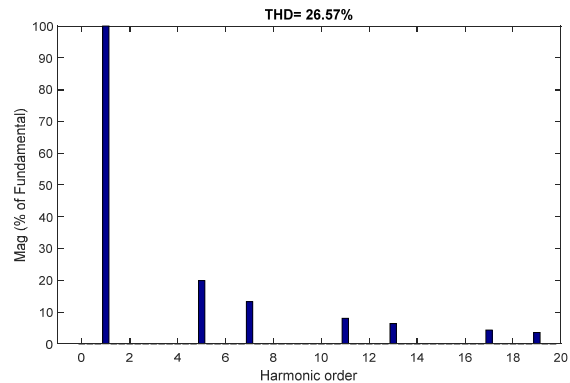
Fig. 7 Current wave I_{sa} before filtering

Fig. 8 Current spectrum in the network before filtering

b. After Application of the Shunt Active Filter Controlled by Hysteresis

After filtering the current I_{sa} by the active shunt filter controlled by conventional hysteresis, we obtain the signal in Fig. 9. We observe a significant improvement in the waveform which has become sinusoidal and whose spectrum given in Fig. 10 allowing us to affirm that there is a clear decrease in harmonics, i.e. a THD of 3.12%.

c. After Application of the MRC-Controlled Active Shunt Filter

By applying the control by Modulation with DCM to our active shunt filter we obtain the signal I_{sa} in Fig. 11 which shows a significant improvement in the curve and whose

current spectrum I_{sa} in Fig. 12 shows a greater reduction in harmonics, i.e. THD = 2.82%.

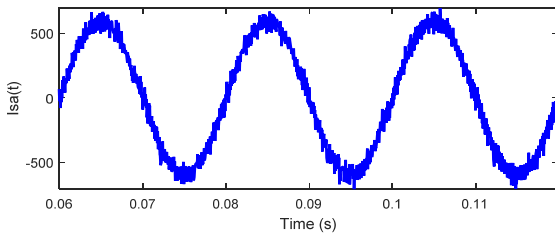


Fig. 9 Current wave I_{sa} after filtering for conventional hysteresis control

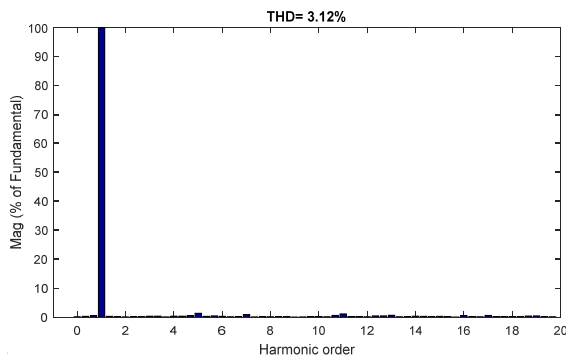


Fig. 10 Current spectrum I_{sa} after filtering for conventional hysteresis control

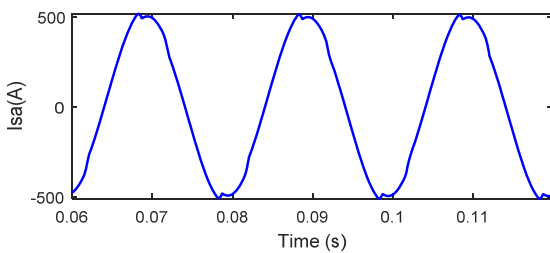


Fig. 11 Current wave I_{sa} after filtering for the DCM command

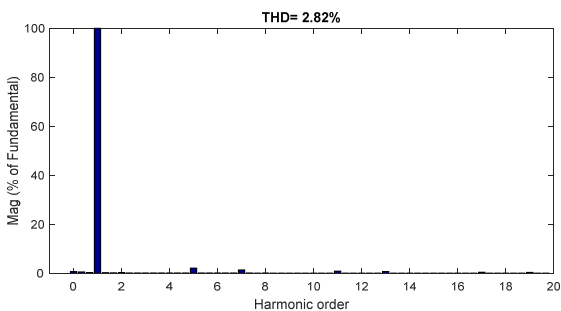


Fig. 12 I_{sa} current spectrum after filtering for DCM control

B. Discussion

Table II gives an interpretation of the results obtained for Hysteresis and Cyclic Ratio Modulation (DCM) control.

THD of the current at phase (a) I_{sa} after filtering calculated on the first 20 harmonic ranks is 3.12% for Hysteresis control

and 2.82% for MRC control, which corresponds to the IEEE-519 standard that limits the THD < 5%, but it can be seen that control by DCM has better performance in terms of harmonic elimination, it is easy to use, ensures operation at a fixed frequency and is also structurally sound.

TABLE II
INTERPRETATION OF PERFORMANCE FOR THE TWO ORDERS

	Hysteresis Control	DCM Control
Waveform of output current	Fairly good	Fairly good
TDH before filtering	26,57%	26,57%
TDH after filtering	3,12%	2,82%
Signal quality	Bruite	No noise
Controllability of the switching frequency	Bad	Good

The performance of the proposed active shunt filter control strategy was compared with the control strategy adopted with some other control methods proposed in the literature. Table III shows the comparison of various control techniques proposed in the literature for harmonic reduction. It is clearly established that all these methods give a THD < 5% thus complying with the IEEE-519 standard, but the control strategy using DCM with the shunt active filter topology proposed in this work is more flexible due to its simplicity of implementation and allows good controllability of the switching frequency of the inverter switches that make up the active filter.

TABLE III
COMPARISON OF METHODS IN THE LITERATURE

Methods for identifying and extracting reference currents and method for monitoring currents	Modified Instantaneous Power Method and Hysteresis Control [7]	P-Q method and Hysteresis control [21]	Three-phase method and DCM control
TDH before filtering	26,5%	27,82%	26,57%
TDH after filtering	2,23%	4,4%	2,82%
Mains voltage	230V	230V	230V
Controllability of the switching frequency	Bad	Bad	Good
Waveform of the current after filtering	Fairly good	Fairly good	Fairly good

IV. CONCLUSION

In this paper we presented the three-monophase method for the identification of disturbance currents, a Simulink model of this method was given and designed the Hysteresis and DCM controls to control the switching commands of the switches of the active shunt filter and then made a comparative study of the two control strategies with those used in the literature. After simulation of the two controls, the results obtained in terms of harmonic reduction comply with the IEEE-519 standard, but it can be seen that the DCM control has better performance in terms of harmonic elimination and is positioned in the literature as a promising method due to its flexibility and ease of implementation in industrial applications. It will be of interest to extend this control strategy to control applications of Current-Structured Inverters

and this could be the subject of future work.

REFERENCES

- [1] Mamane Adamou et al, "Dépollution harmonique des réseaux électriques: Etude comparative des commandes, par Modulation de Largeur d'Impulsion et par Hystérésis, des filtres actifs shunts triphasés," International Journal of Innovation and Applied Studies ISSN 2028-9324, Vol. 28, 2020, pp. 557-566.
- [2] M. Abdusalam, P. Poure and S. Saadate, "A new control scheme of hybrid active filter using Self-Tuning-Filter," Powereng, International Conference on Power Engineering, Energy and Electrical Drives, Setubal, Portugal, 2007.
- [3] A. F. Hanna. Nohra, M. Fadel and H. Y. Kanaan, "A novel instantaneous power based control method for a four-wire SAPF operating with highly perturbed mains voltages," 2016 IEEE International Conference on Industrial Technology (ICIT), Taipei, Taiwan, 2016 pp. 1236-1241.
- [4] Shraddha Dhumal, Jalaja Gundi Poonam Khrid, Manashri Yadav, M.D. Tuljapurkar, "Detection of Harmonics in distribution System using FFT with case studies," International Journal for Scientific Research and Development, 2015, Vol.3 Issue 04, pp 75-82.
- [5] Farooq Haroon, Chengke Zhou, Mohamed Emad Farrag, "Analysing the harmonic distortion in a distribution system caused by the non-linear residential loads," International Journal of Smart Grid and Clean Energy, 2013, Vol. 2, Issue, pp. 46-51.
- [6] T.P Nna Nna, S. Ndjakomo Essiane, S. Pérabi Ngoffé "Control of an Active Filter by Duty Cycle Modulation (DCM) for the Harmonic Decontamination of a Three-Phase Electrical Network" Journal of Power and Energy Engineering, 2020, Vol.8, pp. 1-14.
- [7] M. Abdusalam "Structures et stratégies de commande des filtres actifs parallèles et hybrides avec validations expérimentales" Thèse de doctorat, Université Henri Poincaré-Nancy I France 2008.
- [8] Chaoui Abdelmadjid, "Filtrage actif triphasé pour charges non linéaires," thèse de doctorat L'université de setif, 2010.
- [9] A. Morsli et al "Dépollution des réseaux électriques basse tension utilisant un filtre actif parallèle à deux niveaux contrôlé par l'algorithme P-Q," Médiamira Science, 2012, Vol.53, pp. 105-111.
- [10] A. L. Dourari, M. K. Fellah "Application d'un Filtre Actif Parallèle au Contrôle de la Tension d'un Réseau à Haute Tension, " Conférence Nationale sur la Haute Tension, Laghouat, ALGERIE, Avril 2013.
- [11] Makawana Mukundkumar M., Swapnil Arya "Design of Active Shunt Filter for Harmonics Reduction at Load Side for Power Quality Improvement," International Conference & Expo on "Advances in Power Generation from Renewable Energy Sources APGRES 2017.
- [12] R. Senthil kumar et al, "Reduction and Elimination of Harmonics using Power Active Harmonic Filter," International Journal of Recent Technology and Engineering (IJRTE) ISSN: 2277-3878, Volume-8, Issue-2S3, July 2019.
- [13] Mbihi, J., Ndjali Beng, F., Mbouenda, M., "Modeling and simulation of a class of duty-cycle modulators for industrial instrumentation," Iranian Journal of Electrical and Computer engineering, 4 (2)2, pp. 121-128, 2005.
- [14] Mbihi, J., Ndjali Beng, F., Kom, M., and Nneme Nneme, L. "A novel analog-to-digital conversion technique using nonlinear duty-cycle modulation," International Journal of electronics and computer science engineering, 1(3), pp. 818-825, 2012.
- [15] Mbihi, J., Nneme Nneme, L. "A novel control scheme for buck power converters using duty-cycle modulation," International Journal of power electronics and computer science engineering, 5(3), pp. 185-199, 2013.
- [16] Moffo Lonla B., Jean Mbihi, Leandre Nneme Nneme, "A Low Cost and High Quality Duty-Cycle Modulation Scheme and Applications," International Journal of Electrical, Computer, Energetic, Electronic and communication Engineering, 8(3):82p-88p, 2014.
- [17] A. Obono Biyobo, L. Nneme Nneme, J. Mbihi "A Novel Sine Duty-Cycle Modulation Control Scheme for Photovoltaic Single-Phase Power Inverters," Wseas Transactions on Circuits and Systems, Vol. 17, 2018.
- [18] Liva Falisoa Rafanotsimiva, Gildas Besançon, Didier Georges, Eric Jean Roy Sambatra et Jean Marie Razafimahenina, "Modélisation multimodèle et commande par compensation parallèle distribuée d'un système SMIB," Mada-ENELSA, 2013, Vol. 1, pp. 9-14.
- [19] Gupta Shuvashis Das, Raihan Faruq, Ashraful Bari Chowdhury "A comparative study on harmonics of different electric Bulbs," American Journal of Engineering Research (AJER), 2016, Vol. 5, pp. 156-166.
- [20] G. Sonfack, J. Mbihi, B. Lonla Moffo, "Optimal Duty Cycle Modulation Scheme for Analog-To-Digital Conversion Systems," International Journal of Electronics and Communication Engineering, 2017, Vol.1, pp. 354-360.
- [21] R. Senthil kumar et al "Reduction and Elimination of Harmonics using Power Active Harmonic Filter," International Journal of Recent Technology and Engineering (IJRTE). ISSN: 2277-3878, Vol.8, Issue-2S3, July 2019.